Polarization signal of distant clusters and reconstruction of primordial potential fluctuations

Naoki Seto and Misao Sasaki
Department of Earth and Space Science, Osaka University, Toyonaka 560-0043, Japan
(Received 21 July 2000; published 27 November 2000)

We examine the polarization signal of the cosmic microwave background radiation associated with distant clusters. The polarization is induced by the Thomson scattering of microwave photons with ionized gas of clusters and contains information of quadrupole temperature anisotropies observed at the clusters. The three-dimensional map of the signal is expressed in terms of the spin-weighted harmonics for its angular dependence. Its radial dependence is expanded perturbatively with respect to the distances (equivalently redshifts) to the clusters. The independent information that we can extract from the map is clarified explicitly.

PACS number(s): 98.70.Vc

I. INTRODUCTION

The reconstruction of large-scale density fluctuations is an important topic in modern cosmology. Nowadays there are mainly two methods for this reconstruction. The redshift surveys of galaxies probe the density (more strictly the number density of galaxies) fluctuations around our local (nearby) universe. The anisotropies of the cosmic microwave background (CMB) contain information of potential fluctuations at the last scattering surface (LSS). The redshift survey has been extended deeper and deeper into the universe and has brought us enormous information on the three-dimensional matter distribution. On the other hand, the CMB data, although carrying information of the deepest universe, are of a two-dimensional nature as they are. It therefore would be very interesting to explore the possibilities of extracting out three-dimensional information of primordial fluctuations around the LSS.

The linear polarization of the CMB is induced at a cluster of galaxies by Thomson scattering of CMB photons with the ionized gas (electron) of the cluster [1,2]. The polarization signal is related to one component of the CMB quadrupole moment observed at the cluster. Using this fact, Sazonov and Sunyaev [3] predicted the linear polarization signal of nearby clusters with approximations that the temperature anisotropies observed at these clusters are the same as that observed at our galaxy. They used quadrupole moment of CMB measured by the Cosmic Background Explorer satellite [4].

As pointed out by Kamionkowski and Loeb [5], the LSS of an observer (cluster) depends on the position of the observer. Therefore the LSS of a distant cluster is shifted from our LSS and its polarization signal would probe three-dimensional information of potential fluctuations around our LSS.[1] Kamionkowski and Loeb noticed this effect and commented that the polarization signal of clusters might be used to reduce the cosmic variance limitation of large-scale power spectrum.

Considering further the shift of LSS mentioned above, we can expect that correction terms in the polarization signal proportional to the redshift of clusters $\propto z$ would reflect the first radial derivative of the potential fluctuations at our LSS. In the same manner the signal proportional to the square of redshift $\propto z^2$ would reflect the second radial derivative and so on. In this paper we calculate the three-dimensional map of polarization signal induced by the quadrupole temperature anisotropies of CMB at distant clusters (see also Refs. [6–8]). Then we clarify the information we can extract out from the map. There are many astrophysical or cosmological effects on the polarization of the CMB, such as, the peculiar velocities of clusters or reionization of the universe (see, e.g., Refs. [3,5]). We do not go into these issues but investigate a basic problem about reconstruction of the primordial potential fluctuations from the quadrupole anisotropies of CMB observed at distant clusters.

II. FORMULATION

A. Polarization induced by the Thomson scattering

Polarization of CMB in the direction of a cluster reflects the temperature anisotropy of CMB observed at the cluster. In this subsection we briefly review this effect following Kosowsky [2]. Let us consider a nearly monochromatic plane electromagnetic wave propagating to the z direction. We denote its electric field as

$$E_x = a_x(t)\cos[\omega_0 t - \theta_x(t)], \quad E_y = a_y(t)\cos[\omega_0 t - \theta_y(t)]. \tag{1}$$

Here the amplitudes $a_x(t)$, $a_y(t)$ and the phases $\theta_x(t)$, $\theta_x(t)$ are nearly constant in the oscillation time scale ω_0^{-1} of the wave. The Stokes parameters characterize the polarization of radiation field and are defined as follows (Chandrasekhar [9], Rybicki and Lightman [10])

$$I = \langle a_x^2 \rangle + \langle a_y^2 \rangle, \tag{2}$$

$$Q = \langle a_x^2 \rangle - \langle a_y^2 \rangle, \tag{3}$$

$$U = \langle 2 a_x a_y \cos(\theta_x - \theta_y) \rangle, \tag{4}$$

$$V = \langle 2 a_x a_y \sin(\theta_x - \theta_y) \rangle, \tag{5}$$

where angle brackets represent time averages.

[1] The LSS of a distant cluster is also smaller than ours due to the light-cone effect.

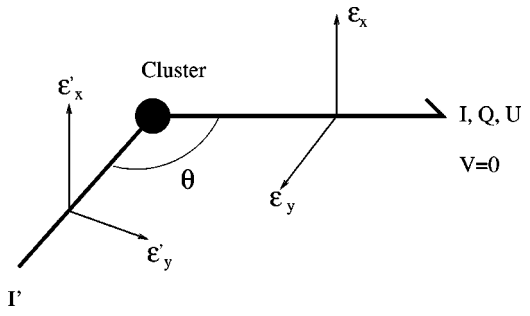

FIG. 1. The Thomson scattering of the CMB photon with ionized gas of a cluster. Initially unpolarized radiation becomes polarized by the quadrupole anisotropy of the incident wave I'.

Next we calculate the polarization induced by the Thomson scattering. The cross section of this process is determined by the polarization vector of the incident wave $\hat{\epsilon}'$ and that of the scattered wave $\hat{\epsilon}$ as [9]

$$\frac{d\sigma}{d\Omega}=\frac{3\sigma_T}{8\pi}|\hat{\epsilon}\cdot\hat{\epsilon}'|^2, \tag{6}$$

where σ_T is the Thomson cross section (Fig. 1). When the incident wave is natural ($Q=U=0$), it is completely described by the angular dependence of the intensity $I'(\theta,\phi)$. Using the above cross section (6) and transformation of the Stokes parameters under rotation of coordinate systems, we obtain the Stokes parameters I, Q, and U for the scattered wave as

$$I=\frac{3\sigma_T}{16\pi}\int d\Omega(1+\cos^2\theta)I'(\theta,\phi), \tag{7}$$

$$Q=\frac{3\sigma_T}{16\pi}\int d\Omega\,\sin^2\theta\cos(2\phi)I'(\theta,\phi), \tag{8}$$

$$U=-\frac{3\sigma_T}{16\pi}\int d\Omega\,\sin^2\theta\sin(2\phi)I'(\theta,\phi). \tag{9}$$

The parameter V which characterizes the circular polarization remains zero in the Thomson scattering.

Let us consider a cluster of galaxies (as a cloud of ionized gas) whose optical depth τ for the Thomson scattering is much smaller than unity. In this optically thin limit we obtain the total Stokes parameters Q and U that are induced by the cluster by replacing σ_T with the optical depth τ in Eqs. (8) and (9). To evaluate the Stokes parameters we expand the angular dependence of the intensity I' in terms of the spherical harmonics as follows:

$$I'(\theta,\phi)=\sum_{lm}\mathcal{I}'_{lm}Y_{lm}(\theta,\phi). \tag{10}$$

Then Eqs. (8) and (9) become

$$Q=\frac{3\tau}{4\pi}\sqrt{\frac{2\pi}{15}}\,\mathrm{Re}(\mathcal{I}'_{22}),\quad U=-\frac{3\tau}{4\pi}\sqrt{\frac{2\pi}{15}}\,\mathrm{Im}(\mathcal{I}'_{22}), \tag{11}$$

or these are simply combined as

$$Q-iU=\frac{3\tau}{4\pi}\sqrt{\frac{2\pi}{15}}\mathcal{I}'_{22}. \tag{12}$$

Therefore, by measuring the polarization parameters (Q,U) in the direction of a cluster, we can, in principle, measure the quadrupole anisotropy $\mathcal{I}'_{22}$ of the CMB observed at the cluster. In reality the incident waves have some degree of polarization. The primordial contribution at small l is expected to be much smaller than the temperature anisotropy for typical cold dark matter (CDM) models, but the total magnitude can become nonnegligible depending on the reionization history (e.g., Refs. [6,8,11]). Furthermore, one cannot deny the possibility of a large tensor contribution to the CMB quadrupole. In this paper, however, we ignore such contributions and focus on a somewhat fundamental problem; what information of the primordial potential field can we reconstruct by using the quadrupole moment $\mathcal{I}_{22}$ observed at different places?

B. Temperature anisotropies of the CMB

In an optically thin universe after decoupling, propagation of the gauge invariant brightness (temperature) perturbation $\mathcal{I}_s$ on the Newtonian hypersurface is written as (Kodama and Sasaki [12])

$$\frac{d}{d\eta}\{\mathcal{I}_s[\eta,\mathbf{x}(\eta),\boldsymbol{\gamma}]+\Psi[\eta,\mathbf{x}(\eta)]\}=\frac{\partial}{\partial\eta}(\Psi-\Phi), \tag{13}$$

where Ψ and Φ are the Newtonian and spatial curvature perturbation, and $\mathbf{x}(\eta)$ represents the null geodesic of the propagating photon that is parametrized by the conformal time η. The temperature perturbation $\mathcal{I}_s$ is related to the intensity perturbation ΔI as $\mathcal{I}_s=\Delta I/(4I)$.

This equation can be formally integrated and the function $\mathcal{I}_s$ at an epoch η is written in terms of quantities at decoupling $\eta_{\rm dec}$ as

$$\begin{aligned}\mathcal{I}_s[\eta,\mathbf{x}(\eta),\boldsymbol{\gamma}]=&\mathcal{I}_s[\eta_{\rm dec},\mathbf{x}(\eta_{\rm dec}),\boldsymbol{\gamma}]\\&+\Psi[\eta_{\rm dec},\mathbf{x}(\eta_{\rm dec})]-\Psi[\eta,\mathbf{x}(\eta)]\\&+2\int_{\eta_{\rm dec}}^{\eta}\frac{\partial}{\partial\eta'}\Psi[\eta',\mathbf{x}(\eta')]d\eta'.\end{aligned} \tag{14}$$

As the anisotropic pressure perturbation is negligible after decoupling, we have put $\Phi=-\Psi$.

For adiabatic perturbations the large scale behavior of the brightness perturbation $\mathcal{I}$ at decoupling is approximately given by the potential field at the same time (Ref. [13])

$$\mathcal{I}_s[\eta_{\rm dec},\mathbf{x}(\eta_{\rm dec}),\boldsymbol{\gamma}]\simeq-\frac{2}{3}\Psi[\eta_{\rm dec},\mathbf{x}(\eta_{\rm dec})]. \tag{15}$$

This is an efficient approximation to discuss small-l (large angle) temperature anisotropies (e.g., Ref. [14]). Thus we consider two effects for anisotropies $\mathcal{I}_s$ seen at clusters that

are known as (i) the Sachs-Wolfe (SW) effect $\mathcal{T}_{\rm SW}$ and (ii) the integrated-Sachs-Wolfe (ISW) effect $\mathcal{T}_{\rm ISW}$,

$$\mathcal{T}_s = \mathcal{T}_{\rm SW} + \mathcal{T}_{\rm ISW}, \tag{16}$$

$$\mathcal{T}_{\rm SW}[\eta, \mathbf{x}(\eta), \boldsymbol{\gamma}] \equiv \frac{1}{3}\Psi[\eta_{\rm dec}, \mathbf{x}(\eta_{\rm dec})], \tag{17}$$

$$\mathcal{T}_{\rm ISW}[\eta, \mathbf{x}(\eta), \boldsymbol{\gamma}] \equiv 2\int_{\eta_{\rm dec}}^{\eta} \frac{\partial}{\partial \eta'}\Psi[\eta', \mathbf{x}(\eta')]d\eta'. \tag{18}$$

Note that the anisotropy $\mathcal{T}_s(\eta, \mathbf{x}, \boldsymbol{\gamma})$ is defined on the shear-free (Newtonian) hypersurface. Nevertheless, since the coordinate gauge transformation affects only the monopole and dipole components of the anisotropy, our analysis does not depend on the choice of the hypersurface.

C. Transformation of coordinate systems

In this section we discuss the relation between two spherical coordinate systems centered at different places. We consider a homogeneous and isotropic universe whose metric is given by

$$ds^2 = a(\eta)^2[-d\eta^2 + dr^2 + f(r)^2(d\theta^2 + \sin^2\theta d\phi^2)], \tag{19}$$

where the function $f(r)$ depends on the spatial curvature radius B and is defined as

$$f(r) = \begin{cases} B\sin\left[\dfrac{r}{B}\right], & \text{closed model,} \\ r, & \text{flat model,} \\ B\sinh\left[\dfrac{r}{B}\right], & \text{open model.} \end{cases}$$

A null geodesic from (or into) the origin $r=0$ along θ $=$const and $\phi=$const is trivially solved in this coordinate system and calculation of the temperature anisotropy $\mathcal{T}(O', \boldsymbol{\gamma})$ observed at a cluster O' is very easy using a coordinate system centered at O' (hereafter call the O' system). However, the linear potential field Ψ is more informative when it is expressed in terms of the coordinate system centered at the Earth O (the O system). Therefore, we need the relation between the spherical coordinate systems centered at different points O and O'. We denote the position of the cluster $\overrightarrow{OO'} \equiv d\hat{\mathbf{e}}_c$ (d: distance to the cluster).

We first set the direction of $\theta=0$ parallel to the direction of the cluster, $\overrightarrow{OO'}$, both for the two systems. Then, due to the rotational symmetry around the axis $\overrightarrow{OO'}$, we can take the same azimuthal angle ϕ in the two systems.[2] In the following we relate the radial distance R and the angle Θ in the O system with the corresponding r and θ in the O' system.

[2]The direction of $\phi=0$ is arbitrary. See also Sec. II E.

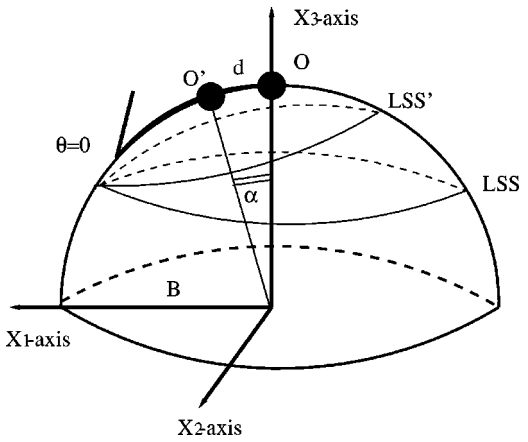

FIG. 2. Correspondence of the two coordinate systems (R, Θ) and (r, θ) centered at different places O and O', respectively. We consider a closed universe with curvature radius B. Two systems coincide with each other by rotation of angle $\alpha \equiv d/B$ around the X_2 axis.

We examine the case of a closed universe, but the results can be straightforwardly extended to flat and open models.

Since the two-dimensional space spanned by (r, θ) with the metric (19) can be embedded in the three-dimensional Euclidean space (X_1, X_2, X_3) as a two-sphere of radius B, the correspondence of the two coordinate systems (R, Θ) and (r, θ) is simply obtained by rotation of the O' system around the X_2 axis with the angle $\alpha \equiv d/B$ (see Fig. 2). Then we obtain the following embedding relation for the three-dimensional coordinates (X_1, X_2, X_3):

$$\frac{X_1}{B} = \sin\frac{R}{B}\cos\Theta = \sin\frac{r}{B}\cos\theta\cos\alpha + \cos\frac{r}{B}\sin\alpha, \tag{20}$$

$$\frac{X_2}{B} = \sin\frac{R}{B}\sin\Theta = \sin\frac{r}{B}\sin\theta, \tag{21}$$

$$\frac{X_3}{B} = \cos\frac{R}{B} = \cos\frac{r}{B}\cos\alpha - \sin\frac{r}{B}\cos\theta\sin\alpha. \tag{22}$$

Using the above, an event (η, R, Θ, ϕ) in the O system can be perturbatively expressed in terms of the corresponding event (η, r, θ, ϕ) in the O' system as

$$\eta = \eta,$$

$$R = r + d\cos\theta + O(d^2),$$

$$\Theta = \theta - \frac{d}{B}\sin\theta\cot\frac{r}{B} + O(d^2),$$

$$\phi = \phi. \tag{23}$$

Here we have assumed $r \gg d$. This assumption formally breaks down when we calculate the ISW contribution near the cluster (see the next section). Nevertheless, this contribu-

tion is found to be negligible at the d^1-st order for $\eta_0 - \eta_{\rm dec} \gg d$, where η_0 is the conformal time at present.

Using the above equations (23), the potential perturbation $\Psi_{O'}(\eta,r,\theta,\phi;\hat{\mathbf{e}}_c)$ in the O' system is expressed in terms of that in the O system as

$$\begin{aligned}\Psi_{O'}(\eta,r,\theta,\phi;\hat{\mathbf{e}}_c) &= \Psi_O[\eta,R(r,\theta),\Theta(r,\theta),\phi] \\ &= \Psi_O(\eta,r,\theta,\phi;\hat{\mathbf{e}}_c) + \partial_r \Psi_O(\eta,r,\theta,\phi;\hat{\mathbf{e}}_c) \\ &\quad \times [R(r,\theta)-r] + \partial_\theta \Psi_O(\eta,r,\theta,\phi;\hat{\mathbf{e}}_c) \\ &\quad \times [\Theta(r,\theta)-\theta] + O(d^2). \end{aligned} \tag{24}$$

D. Quadrupole moment at a cluster

In Sec. II A, we have discussed the relation between the polarization and temperature anisotropies. Here we calculate the quadrupole anisotropy of CMB at a cluster O' which is observed as the Stokes parameter $Q-iU$ in the direction from the Earth O. The quadrupole mode $\mathcal{T}_{22}$ seen at the cluster O' is written as

$$(Q-iU) \propto \mathcal{X}(\hat{\mathbf{e}}_c,d) \equiv \int \mathcal{T}(\eta_0-d, d\hat{\mathbf{e}}_c, \boldsymbol{\gamma}) Y^*_{22}(\boldsymbol{\gamma};\hat{\mathbf{e}}_c) d\Omega_{\boldsymbol{\gamma}}, \tag{25}$$

where we have explicitly denoted the orientation of the polar axis $\hat{\mathbf{e}}_c$ to show our specific choice of the coordinate assigned for each cluster O'.

The large angle (small l) temperature anisotropies are dominated by the Sachs-Wolfe effect and the integrated Sachs-Wolfe effect. The Sachs-Wolfe effect is written in terms of the potential field Ψ in the O' coordinates as

$$\mathcal{T}_{\rm SW}(\eta_0-d, d\hat{\mathbf{e}}_c, \boldsymbol{\gamma}) = \frac{1}{3}\Psi_{O'}[\eta_{\rm dec}, (\eta_0-d-\eta_{\rm dec})\boldsymbol{\gamma}]. \tag{26}$$

With Eqs. (24), (25), and (26) we can evaluate the quadrupole mode $\mathcal{X}_{\rm SW}$ due to the SW effect.

To evaluate the integral (25) we expand the linear potential field Ψ in the O system by the spherical harmonics as

$$\Psi_O(\eta,r,\theta,\phi;\hat{\mathbf{e}}_c) = \sum_{lm} F(\eta)\Psi_{lm}(r;\hat{\mathbf{e}}_c) Y_{lm}(\theta,\phi;\hat{\mathbf{e}}_c). \tag{27}$$

Here the function $F(\eta)$ represents the time dependence of the linear potential fluctuation and is proportional to D/a (D is the linear growth rate of density contrast). In the case of the Einstein–de Sitter universe or at an early matter-dominated stage of general models, we have $D/a = \text{const}$ [15]. Thus we fix $D/a=1$ at $\eta=\eta_{\rm dec}$ and normalize the time dependence by $F(\eta_{\rm dec})=1$.

After some algebra we obtain the following result:

$$\begin{aligned}\mathcal{X}_{\rm SW}(\hat{\mathbf{e}}_c,d) &= \frac{\Psi_{22}(\eta_0;\hat{\mathbf{e}}_c)}{3} + \frac{1}{3}d\Bigg[-\Psi'_{22}(\eta_0;\hat{\mathbf{e}}_c) \\ &\quad + \frac{1}{\sqrt{7}}\Psi'_{32}(\eta_0;\hat{\mathbf{e}}_c) \\ &\quad + \frac{4}{\sqrt{7}B}\Psi_{32}(\eta_0;\hat{\mathbf{e}}_c)\cot\frac{\eta_0}{B}\Bigg] + O(d^2), \end{aligned} \tag{28}$$

where the prime denotes the radial derivative and we have put $\eta_0 - \eta_{\rm dec} = \eta_0$ (since $\eta_{\rm dec} \ll \eta_0$), and have used formulas for the spherical harmonics such as

$$\cos\theta Y_{22}(\theta,\phi) = \frac{1}{\sqrt{7}} Y_{32}(\theta,\phi). \tag{29}$$

Similarly the quadrupole mode induced by the integrated-Sachs-Wolfe effect is written as

$$\begin{aligned}\mathcal{X}_{ISW}(\hat{\mathbf{e}}_c,d) &= 2\|\Psi'_{22}(\eta;\hat{\mathbf{e}}_c)\| + 2d\Bigg(-\|\Psi'_{22}(\eta;\hat{\mathbf{e}}_c)\| \\ &\quad + \frac{1}{\sqrt{7}}\|\Psi'_{32}(\eta;\hat{\mathbf{e}}_c)\| \\ &\quad + \frac{4}{\sqrt{7}B}\left\|\Psi_{32}(\eta;\hat{\mathbf{e}}_c)\cot\frac{\eta}{B}\right\|\Bigg) + O(d^2), \end{aligned} \tag{30}$$

where we have defined an integral operator $\|\cdots\|$ as

$$\|y(\eta)\| \equiv \int_0^{\eta_0} F'(\eta_0-\eta) y(\eta) d\eta. \tag{31}$$

The d^0-th order term is essentially the same as the result obtained in Eq. [3]. The formulas (28) and (30) are easily extended to general background geometry. We obtain the formulas for the flat universe in the limit $B\to\infty$ and for the open universe by replacement $\cot[x]\to\coth[x]$.

In the Einstein–de Sitter Universe the ISW effect vanishes ($F'=0$) and the quadrupole moment is determined solely by the three-dimensional information of the potential field Ψ at the decoupling. In this case, we have the following result up to the second order of d:

$$\begin{aligned}3\mathcal{X}(\hat{\mathbf{e}}_c,d) &= \Psi_{22} + d\left(-\Psi'_{22} + \frac{1}{\sqrt{7}}\Psi'_{32} + \frac{4}{\sqrt{7}}\frac{\Psi_{32}}{\eta_0}\right) \\ &\quad + d^2\Bigg(\frac{4}{7}\Psi''_{22} + \frac{1}{7\eta_0}\Psi'_{22} - \frac{3}{7\eta_0^2}\Psi_{22} - \frac{1}{\sqrt{7}}\Psi''_{32} \\ &\quad - \frac{4}{\sqrt{7}\eta_0}\Psi'_{32} + \frac{4}{\sqrt{7}\eta_0^2}\Psi_{32} + \frac{1}{7\sqrt{3}}\Psi''_{42} \\ &\quad + \frac{3\sqrt{3}}{7\eta_0}\Psi'_{42} + \frac{5\sqrt{3}}{7\eta_0^2}\Psi_{42}\Bigg) + O(d^3), \end{aligned} \tag{32}$$

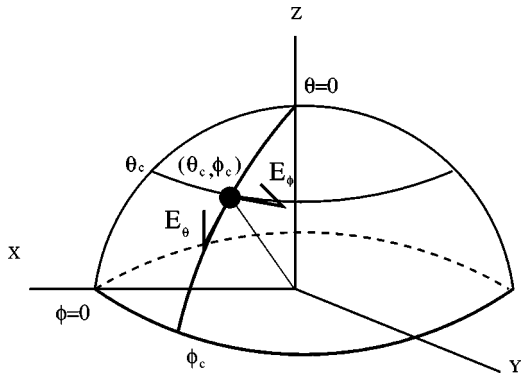

FIG. 3. Relation between the coordinate system specific to each cluster and the Earth fixed coordinate system.

where we have denoted $\Psi_{lm}(\eta_0;\hat{\mathbf{e}}_c)$ by Ψ_{lm} for simplicity.

E. All sky map and reconstruction of the linear potential field

The result given in the previous subsection depends on the specific choice of the coordinate system defined for each cluster. We have set the direction of $\theta=0$ toward the direction of the cluster $\hat{\mathbf{e}}_c \propto \overrightarrow{OO'}$. Here in order to consider an all sky map of the quadrupole moments seen at clusters, we express the coefficient $\Psi_{lm}(r;\hat{\mathbf{e}}_c)$ in terms of the harmonic coefficients for a spherical coordinate system fixed at the Earth. We denote the direction of a cluster $\hat{\mathbf{e}}_c$ in this fixed coordinate as (see Fig. 3)[3]

$$\hat{\mathbf{e}}_c=(\sin\theta_c\cos\phi_c,\sin\theta_c\sin\phi_c,\cos\theta_c), \tag{33}$$

and the linear potential field as

$$\Psi(\eta,r,\theta,\phi)=\sum_{lm} F(\eta)\Psi_{lm}(r)Y_{lm}(\theta,\phi). \tag{34}$$

The relation between the two coefficients $\Psi_{lm}(r;\hat{\mathbf{e}}_c)$ and $\Psi_{lm}(r)$ is given by the two successive rotations of the system by $\mathbf{R}_z(-\phi_c)$ and $\mathbf{R}_y(-\theta_c)$, where $\mathbf{R}_a(\alpha)$ is the rotation operator around the a axis with angle α:

$$\Psi_{l2}(r;\hat{\mathbf{e}}_c)=\langle l2|\mathbf{R}_y(-\theta_c)\mathbf{R}_z(-\phi_c)|\Psi(r,\theta,\phi)\rangle \tag{35}$$

$$=\sum_{l'm'}\langle l2|\mathbf{R}_y(-\theta_c)\mathbf{R}_z(-\phi_c)|l'm'\rangle \times\langle l'm'|\Psi(r,\theta,\phi)\rangle \tag{36}$$

$$=\sum_{m'}\sqrt{\frac{4\pi}{2l+1}}\Psi_{lm'}(r)\,{}_{-2}Y_{lm'}(\theta_c,\phi_c). \tag{37}$$

[3]We choose the direction of $\phi=0$ in the O' system parallel to $\mathbf{E}_\theta$ in Fig. 3.

Here we have followed the notation of Sakurai [16]. Namely, the ket-vector $|f\rangle$ represents an angular function $f(\theta,\phi)$ and bra-vector $\langle f|$ its complex conjugate. The inner product denotes the angular integrals

$$\langle g|f\rangle\equiv\int_0^{2\pi}d\phi\int_0^{\pi}d\theta\sin\theta g^*(\theta,\phi)f(\theta,\phi). \tag{38}$$

The function ${}_{-s}Y_{lm}(\theta,\phi)$ in Eq. (37) is the spin-weighted spherical harmonic [17] and is given in terms of the rotation matrix of the scalar spherical harmonic $|lm\rangle\equiv Y_{lm}$ as

$${}_{-s}Y_{lm}(\theta,\phi)\equiv\sqrt{\frac{2l+1}{4\pi}}\langle ls|\mathbf{R}_y(-\theta)\mathbf{R}_z(-\phi)|lm\rangle. \tag{39}$$

Thus the all sky (three-dimensional) map of $\mathcal{X}=\mathcal{X}_{\rm SW}+\mathcal{X}_{\rm ISW}$ is expressed in terms of the coefficients Ψ_{lm} defined on a fixed coordinate system as

$$\begin{aligned}\mathcal{X}_{\rm SW}(\hat{\mathbf{e}}_c,d)=&\sqrt{\frac{4\pi}{45}}\,{}_{-2}Y_{2m}(\theta_c,\phi_c)\Psi_{2m}(\eta_0)\\&+d\Bigg[-\sqrt{\frac{4\pi}{45}}\,{}_{-2}Y_{2m}(\theta_c,\phi_c)\Psi'_{2m}(\eta_0)\\&+\frac{\sqrt{4\pi}}{21}\left(\Psi'_{3m}(\eta_0)+\frac{4}{B}\Psi_{3m}(\eta_0)\cot\frac{\eta_0}{B}\right)\\&\times\,{}_{-2}Y_{3m}(\theta_c,\phi_c)\Bigg]+O(d^2)\end{aligned} \tag{40}$$

and

$$\begin{aligned}\mathcal{X}_{\rm ISW}(\hat{\mathbf{e}}_c,d)=&2\sqrt{\frac{4\pi}{5}}\,{}_{-2}Y_{2m}(\theta_c,\phi_c)\|\Psi_{2m}(\eta)\|\\&+2d\Bigg[-\sqrt{\frac{4\pi}{5}}\,{}_{-2}Y_{2m}(\theta_c,\phi_c)\|\Psi'_{2m}(\eta)\|\\&+\frac{\sqrt{4\pi}}{7}\left(\|\Psi'_{3m}(\eta)\|+\frac{4}{B}\left\|\Psi_{3m}(\eta)\cot\frac{\eta}{B}\right\|\right)\\&\times\,{}_{-2}Y_{3m}(\theta_c,\phi_c)\Bigg]+O(d^2).\end{aligned} \tag{41}$$

Assuming that we have the all sky map of $\mathcal{X}$, we can extract out information of Ψ_{lm} for each (l,m) mode by using the orthonormal relation for the spin-weighted harmonics

$$\int_0^{2\pi}d\phi\int_0^{\pi}d\theta\sin\theta\,{}_{-s}Y^*_{lm}(\theta,\phi)\,{}_{-s}Y_{l'm'}(\theta,\phi)=\delta_{l'l}\delta_{m'm}. \tag{42}$$

From Eqs. (40) and (41), we see that by observing the d dependence (or equivalently the linear redshift dependence) of the polarization map, we obtain information of the linear potential fluctuations in the combination

$$-\sqrt{\frac{4\pi}{45}}\Psi'_{2m}(\eta_0)-2\sqrt{\frac{4\pi}{5}}\|\Psi'_{2m}(\eta_0)\|, \tag{43}$$

for $l=2$ modes and

$$\frac{\sqrt{4\pi}}{21}\left(\Psi'_{3m}(\eta_0)+\frac{4}{B}\Psi_{3m}(\eta_0)\cot\frac{\eta_0}{B}\right) + \frac{\sqrt{4\pi}}{7}\left(\|\Psi'_{3m}(\eta)\|+\frac{4}{B}\left\|\Psi_{3m}(\eta)\cot\frac{\eta}{B}\right\|\right), \tag{44}$$

for $l=3$ modes.

In the case of the Einstein–de Sitter universe, the multipole components $\Psi_{lm}(\eta_0)$ for small l at the last scattering surface $r=\eta_0$ can be obtained directly from the temperature anisotropies $\mathcal{T}$. If we have the polarization map we can further obtain the following information: From the $O(d)$ map and the temperature anisotropy $\mathcal{T}$, we obtain

$$\Psi'_{2m}(\eta_0), \quad \Psi'_{3m}(\eta_0), \tag{45}$$

and from the polarization map up to $O(d^2)$ order and the temperature anisotropy $\mathcal{T}$,

$$\Psi''_{2m}(\eta_0), \quad \Psi''_{3m}(\eta_0), \quad 9\frac{\Psi'_{4m}(\eta_0)}{\eta_0}+\Psi''_{4m}(\eta_0). \tag{46}$$

Note that we cannot separate $\Psi'_{4m}(\eta_0)$ from $\Psi''_{4m}(\eta_0)$. Using information of the polarization up to the d^n (or z^n) order we would know the derivative coefficients $\partial^i_{\eta_0}\Psi_{2m}(\eta_0)$ and $\partial^i_{\eta_0}\Psi_{3m}(\eta_0)$ separately for $i\leqslant n$ but not for $l\geqslant 4$ modes.

So far we have inquired a basic problem of reconstruction, considering an idealistic and simplified situation. Here we have to mention two points that would be important to apply our reconstruction method to real observational data. The first point is that the polarization signal $Q-iU$ of a cluster is obtained by a combination of the temperature anisotropy $\mathcal{T}_{22}$ at the cluster and its optical depth τ, as shown in Eq. (12). We have implicitly assumed that we can separate them. This could be achieved, for example, by using x-ray and thermal Sunyaev-Zeldovich data. The second point is that distribution of clusters is not homogeneous on our light cone (both in redshift and angular position). To extract out information of the potential field from inhomogeneous sample of clusters it would be necessary to develop a workable statistical method.

III. EXAMPLES

As shown in the previous section the polarization signal contains both the SW and ISW effects. The former reflects local quantity at the last scattering surface and more interesting from the point of reconstructing the linear potential field Ψ.

In this section we calculate the magnitude of these two effects for concrete models. We investigate flat cold-dark-matter (CDM) models with cosmological constant λ_0 ($\Omega_0+\lambda_0=1$). We use the primordially Harrison-Zeldovich spectrum with the CDM transfer function given in Bardeen et al. [18]. The Hubble parameter is fixed at $h=0.7$ (h is the Hubble parameter in units of 100 km/sec/Mpc). The shape parameter Γ of the CDM transfer function is set at $\Gamma=h\Omega_0$.

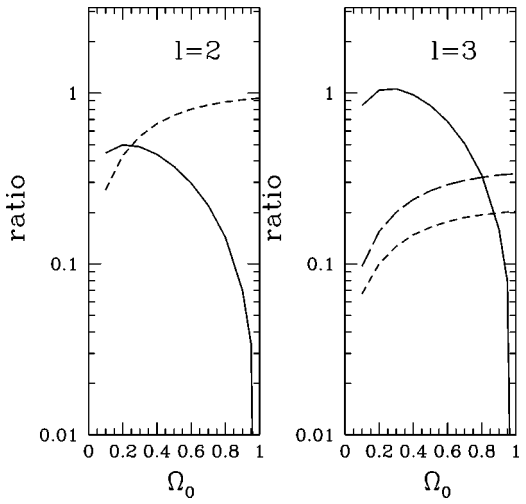

FIG. 4. Ratio of the d^1-st order polarization signal and the d^0-th signal for a cluster at $z=0.5$. We consider flat CDM models with cosmological constant. The dashed lines represent the contribution of the SW effect and the solid of the ISW effect. For $l=3$ modes, there are two SW terms. The long-dashed line represents the term proportional to Ψ and the short-dashed line the term proportional to Ψ'.

We first calculate the rms value for the d^0-th signal of $\mathcal{X}$ [Eqs. (40) and (41)],

$$-\sqrt{\frac{4\pi}{45}}\Psi_{2m}(\eta_0)-2\sqrt{\frac{4\pi}{5}}\|\Psi_{2m}(\eta_0)\|, \tag{47}$$

and the same quantities for the d^1-st order correction for $l=2$ mode both for the SW and ISW effects [Eq. (43)]

$$-\sqrt{\frac{4\pi}{45}}\Psi'_{2m}(\eta_0), \quad -2\sqrt{\frac{4\pi}{5}}\|\Psi'_{2m}(\eta_0)\|. \tag{48}$$

For $l=3$ mode at the d^1-st order the SW effect is constituted by two terms [Eq. (44)] and we treat them separately. We evaluate the rms values of the three quantities

$$\frac{\sqrt{4\pi}}{21}\Psi'_{3m}(\eta_0), \quad 4\frac{\sqrt{4\pi}}{21\eta_0}\Psi_{3m}(\eta_0), \quad \frac{\sqrt{4\pi}}{7}\left(\|\Psi'_{3m}(\eta)\|+4\left\|\frac{\Psi_{3m}(\eta)}{\eta}\right\|\right). \tag{49}$$

In Fig. 4 we plot the ratio of the d^1-st signal at $z=0.5$ to the d^0-th signal. First, note that the magnitude of the d^1-st correction is significant even at $z=0.5$. For $l=2$ mode the SW effect is larger than the ISW effect for $\Omega_0\gtrsim 0.3$ and the d^1-st signal becomes comparable to the d^0-th signal for $\Omega_0\simeq 1.0$. For $l=3$ modes, the Ψ_{3m} contribution to the SW effect is

larger than the Ψ'_{3m} contribution. Here the ISW effect is stronger than the case of $l=2$ and the SW effect becomes dominant only for $\Omega_0 \gtrsim 0.8$.

IV. SUMMARY

The polarization signal of CMB associated with a distant cluster reflects temperature anisotropies observed at the cluster. Using this effect we can, in principle, obtain three-dimensional information of potential fluctuations around the last scattering surface (LSS). In this paper we have calculated the three-dimensional map of the polarization signal of clusters induced by the temperature anisotropies in homogeneous and isotropic background universe. We have considered adiabatic scalar perturbations and included both the Sachs-Wolfe effect and the integrated-Sachs-Wolfe effect. Our formulation is valid for general background geometries. The radial part of the three-dimensional map is expressed perturbatively with respect to the distances (or equivalently redshifts) of clusters, and angular dependence is written in terms of the spin-weighted harmonics. Using the orthonormality of the harmonics, the independent information that can be extracted out from the map is clarified explicitly.

In the case of the Einstein–de Sitter universe, the integrated-Sachs-Wolfe effect vanishes and the temperature anisotropies solely probe the local quantities around the LSS. We showed that using the polarization signal up to the z^n-th order, the derivative coefficients $\partial^i_{\eta_0}\Psi_{lm}$ would be separately obtained for $l=2$ and 3 modes. But we cannot separate them for modes with $l \geqslant 4$.

For general background cosmological models the polarization signal also contains the integrated-Sachs-Wolfe effect. In Sec. III we have examined the first (z^1-th) order polarization signal for typical flat CDM models with cosmological constant. We found that the Sachs-Wolfe effect dominates the signal of $l=2$ modes for density parameter $\Omega_0 \gtrsim 0.3$, but it dominates the $l=3$ signals only for $\Omega_0 \gtrsim 0.8$. The integrated-Sachs-Wolfe effect is a nonlocal effect and troublesome from the point of view to reconstruct the primordial potential fluctuations. But it mainly comes from time variation of the potential field at relatively recent epoch. Hence we might be able to separate its effect by probing the large-scale matter distribution with other observational tools (e.g., Ref. [19]).

ACKNOWLEDGMENTS

N.S. would like to thank N. Sugiyama and G.-C. Liu for useful discussions. This work has been supported by the Japanese Grant in Aid for Science Research Fund of the Ministry of Education, Science, Sports and Culture Grant Nos. 01416 (N.S.) and 12640269 (M.S.).

[1] Ya. Zeldovich and R. A. Sunyaev, Sov. Astron. Lett. **6**, 285 (1980).
[2] A. Kosowsky, Ann. Phys. (N.Y.) **246**, 49 (1996).
[3] S. Y. Sazonov and R. A. Sunyaev, Mon. Not. R. Astron. Soc. **310**, 765 (1999).
[4] A. Kogut *et al.*, Astrophys. J. Lett. **464**, 5 (1996).
[5] M. Kamionkowski and A. Loeb, Phys. Rev. D **56**, 4511 (1997).
[6] M. Zaldarriaga and U. Seljak, Phys. Rev. D **55**, 1830 (1997).
[7] M. Kamionkowski, A. Kosowsky, and A. Stebbins, Phys. Rev. D **55**, 7368 (1997).
[8] W. Hu and M. White, Phys. Rev. D **56**, 596 (1997).
[9] S. Chandrasekhar, *Radiative Transfer* (Dover, New York, 1960).
[10] G. B. Rybicki and A. P. Lightman, *Radiative Process in Astrophysics* (Wiley, New York, 1960).
[11] M. Zaldarriaga, Phys. Rev. D **55**, 1822 (1997).
[12] H. Kodama and M. Sasaki, Int. J. Mod. Phys. A **1**, 265 (1986).
[13] R. K. Sachs and A. M. Wolfe, Astrophys. J. **147**, 73 (1967).
[14] N. Gouda, N. Sugiyama, and M. Sasaki, Prog. Theor. Phys. **85**, 1023 (1991).
[15] P. J. E. Peebles, *The Large Scale Structure in the Universe* (Princeton University Press, Princeton, 1980).
[16] J. J. Sakurai, *Modern Quantum Mechanics* (Addison-Wesley, New York, 1985).
[17] E. Newman and R. Penrose, J. Math. Phys. **7**, 863 (1966); J. N. Goldberg *et al.*, *ibid.* **8**, 2155 (1967).
[18] J. M. Bardeen, J. R. Bond, N. Kaiser, and A. Szalay, Astrophys. J. **304**, 15 (1986).
[19] R. G. Crittenden and N. G. Turok, Phys. Rev. Lett. **76**, 575 (1996); A. Kinkhabwala and M. Kamionkowski, *ibid.* **82**, 4172 (1999).